ENERGETIC PROCESSING OF INTERSTELLAR SILICATE GRAINS BY COSMIC RAYS

E. M. BRINGA,[1] S. O. KUCHEYEV,[1] M. J. LOEFFLER,[2] R. A. BARAGIOLA,[2] A. G. G. M. TIELENS,[3] Z. R. DAI,[4]
G. GRAHAM,[4] S. BAJT,[1] J. P. BRADLEY,[4] C. A. DUKES,[2] T. E. FELTER,[1] D. F. TORRES,[5] AND W. VAN BREUGEL[4]

ABSTRACT

While a significant fraction of silicate dust in stellar winds has a crystalline structure, in the interstellar medium nearly all of it is amorphous. One possible explanation for this observation is the amorphization of crystalline silicates by relatively "low" energy, heavy-ion cosmic rays. Here we present the results of multiple laboratory experiments showing that single-crystal synthetic forsterite (Mg_2SiO_4) amorphizes when irradiated by 10 MeV Xe ions at large enough fluences. Using modeling, we extrapolate these results to show that 0.1–5.0 GeV heavy-ion cosmic rays can rapidly ($\sim$70 Myr) amorphize crystalline silicate grains ejected by stars into the interstellar medium.

Subject headings: cosmic rays — dust, extinction

Online material: color figures

1. INTRODUCTION

Interstellar dust grains, while comprising only $\sim$1% of the mass in the interstellar medium, are important, because they catalyze the formation of many gas-phase molecules, in particular, H_2 (Hollenbach & Salpeter 1971), which allow the cooling and collapse of molecular clouds and the formation of stars and planets. High-energy radiation and particles from hot stars, supernovae, or active black holes can alter the physical properties of dust grains and thereby affect their role in these processes. Understanding the composition, characteristics, origin, and evolution of interstellar medium (ISM) dust is thus a key question in astrophysics (Draine 2003).

Most of the dust is formed by condensation in the atmospheres of old stars, which eject a significant fraction of their material back into the ISM. Silicates, such as those producing terrestrial planets, are injected from oxygen-rich asymptotic giant branch (AGB) stars, red supergiants, and supernovae (Tielens 2005). The fraction of crystalline silicates observed in stellar winds covers a large range (0.05–0.75; Sylvester et al. 1999; Molster et al. 1999). The resulting fraction of crystalline silicates injected into the ISM by red giant and supergiant stars is then estimated to be 0.15 (Kemper et al. 2004; Waters 2004). Specifically, the infrared spectra of the red giants and supergiants reveal the spectroscopic signature of the Mg-rich end-members of the olivine and pyroxene families, forsterite (Mg_2SiO_4) and enstatite ($MgSiO_3$). In contrast, the interstellar 9.7 μm silicate feature reveals no evidence for crystalline silicates, and hence, after entering the ISM, crystalline silicates ejected by stellar sources are rapidly amorphized by some mechanism. The upper limit for the crystalline fraction of silicates in the ISM is $\sim$1% (Kemper et al. 2004).

Previous laboratory studies have focused on simulating amorphization of complex silicates by low-velocity shocks, using irradiation with low-energy (keV) ions. Amorphization has been shown in several experiments using 4–50 keV ions at fluences of 10^{15}–10^{17} ions cm^{-2} (Demyk et al. 2001; Jaeger et al. 2003; Brucato et al. 2004). However, this processing is inefficient, because in a 200 km s^{-1} shock (0.2 keV amu^{-1}), the range of the ions is much smaller than the size of most interstellar grains. Ions of much higher energy, which can penetrate even the largest interstellar grains, pervade the ISM in the form of cosmic rays (CRs; >1 MeV $nucleon^{-1}$). However, until now, processing of dust by such swift ions has been dismissed (Day 1977; Brucato et al. 2004; Watson & Salpeter 1972), because it is believed that the accumulated energy deposition by CRs cannot reach the values needed for amorphization (Jaeger et al. 2003; Brucato et al. 2004; Demyk et al. 2004). In this respect, most of the CR flux consists of H and He ions, but MeV He shows no evidence for amorphization of silicates, even for very high ion fluences (Day 1977). However, it is well known that the fluence/energy deposition required for amorphization with keV ions, where elastic atomic interactions dominate, cannot simply be extrapolated to CR energies, where electronic excitations dominate energy deposition (Ziegler 2003). Indeed, while fast light ions such as H and He do not typically form amorphous tracks in silicates, swift heavy ions (such as Fe) do, a phenomenon that has been studied for decades (Fleischer et al. 1975) and applied to dating and advanced material modification. Heavy CRs (Fe) are less abundant in the ISM than light CRs (H, He) by a factor of $\sim$$10^{-4}$ (Wiebel-Sooth et al. 1998 and discussion in our § 4). However, at 1 GeV, an Fe ion deposits $\sim$$10^4$ times more energy per unit path length in silicates (Ziegler 2003) than do protons, and lattice defect formation for swift heavy ion is due to electronic energy loss. Therefore, the cumulative damage in interstellar dust by swift heavy ions can rival or even well exceed that by light ions. Here we demonstrate, using both experiments and modeling, that heavy CR ions are the dominant processing agents of dust in the diffuse ISM.

This paper is organized as follows. First, in § 2 we describe the experimental setup, the choice of the material used, and the methods used to analyze and quantify the results, which are described in § 3. We discuss our findings in § 4, which begins with a critical analysis of why CR processing of Galactic ISM dust is indeed important (§ 4.1). For this we estimate the ISM CR spectrum using a "leaky box" model (§ 4.1.1), and using phenomenological electronic energy deposition models (§ 4.1.2), we demonstrate that our laboratory experiments at 0.08 MeV $nucleon^{-1}$ (but with a large electronic energy loss of $\sim$4.5 keV nm^{-1}) can

[1] Lawrence Livermore National Laboratory, Livermore, CA 94550; ebringa@llnl.gov, wil@igpp.llnl.gov.

[2] Laboratory for Atomic and Surface Physics, University of Virginia, Charlottesville, VA 22903.

[3] NASA Ames Research Center, Moffett Field, CA 94035.

[4] Institute of Geophysics and Planetary Physics, Lawrence Livermore National Laboratory, Livermore, CA 94550.

[5] ICREA and Institut de Ciencies de l'Espai, Campus UAB, 08193 Barcelona, Spain.

be confidently extrapolated to the relevant (relatively low) CR energies at 1–100 MeV nucleon^{-1}, where amorphization is most efficient. We then end this section with estimates of the interstellar dust grain amorphization timescale (§ 4.1.3) and the expected fraction of interstellar crystalline silicates. In the subsequent sections we compare these results with other possible amorphization processes such as ion bombardment by interstellar shocks (§ 4.2), the life cycle of crystalline silicates (§ 4.3), and the amorphization of dust grains in the solar system (§ 4.4) and stellar debris disks (§ 4.5). We then conclude (§ 5) that CR processing of ISM dust is indeed important in our own Galaxy, that it may explain the amorphization of crystalline silicates, and that it is likely to be an even more important effect in forming (starburst) galaxies, which have much higher CR fluxes due to 10–1000 times larger star formation rates and emerging active black holes (Torres et al. 2004).

2. METHOD

To investigate the effects of CRs on crystalline silicates, we irradiated samples of undoped forsterite (Mg_2SiO_4) single crystals with triply ionized, 10 MeV Xe ions. After irradiation with specific fluences, we analyzed these samples using Rutherford-backscattering/channeling (RBS/C) spectrometry, infrared (IR) reflection spectroscopy, and transmission electron microscopy (TEM) of electron transparent cross sections of the irradiated forsterites. In this section, we briefly discuss the experimental techniques.

2.1. Ion Irradiation and RBS/C Spectrometry

The Lawrence Livermore National Laboratory (LLNL) 4 MV ion accelerator was used for ion bombardment and for RBS/C analysis in single alignment conditions. Samples of laboratory-grown undoped forsterite (Mg_2SiO_4) (100) single crystals, $10 \times 10 \times 3$ mm^3 in size, were bombarded at room temperature with 10 MeV $^{132}Xe^{3+}$ ions using a flux of $(1–2) \times 10^{10}$ ions cm^{-2} s^{-1} to a fluence range of 5×10^{11} to 6×10^{13} ions cm^{-2}. Ion incidence was at an angle of $\sim 7°$ relative to the surface normal, to minimize channeling. At this energy, 86% of the total stopping power (energy loss per unit path length) is electronic (4.5 keV nm^{-1}, decreasing with penetration depth as the ion slows down [Ziegler 2003]). Furthermore, in this case the xenon ions have a projected range of ~ 2.4 μm in forsterite (Ziegler et al. 2003) and, hence, can only alter a near-surface layer with thickness close to the projected ion range.

RBS/C (Chu et al. 1978) is a well-established quantitative technique for the analysis of the elemental composition and crystallinity of the surface and the outer few microns of solids. Typically, in RBS/C, a beam of 0.1–3.0 MeV He ions is directed at the sample. The flux and energy distribution of the elastically backscattered particles, measured under a given angle, gives information on the structure of the sample. We characterized all our samples after irradiation by RBS/C with 2 MeV $^4He^+$ ions incident along the (100) direction and backscattered at 164°. Damage buildup curves were analyzed with the defect overlap model of cylindrical tracks (Gibbons 1972), in which, in the simplest case of so-called zero overlap, the relative concentration of defects is $\left[1 - \exp\left(-\pi R_{track}^2 D\right)\right]$, where D is ion fluence and R_{track} is the effective radius of an amorphous track that each impinging ion creates along its path in the crystal. Note that the "bulk" samples used here should require roughly the same amorphization fluence as submicron grains (Bringa & Johnson 2004). However, grains smaller than 10 nm might not only amorphize but might also be destroyed completely by a single CR impact (Bringa & Johnson 2004; Berthelot et al. 2000; Toulemonde et al. 2002).

2.2. Transmission Electron Microscopy: Sample Preparation and Measurements

After ion irradiation, ~ 100 nm thick forsterite sections were prepared using a FEI 237 DualBeam™ focused ion beam (FIB)/field emission scanning electron microscope (FESEM) and FEI Nova 600 DualBeam™ FIB/FESEM instruments (Graham et al. 2004). The extracted cross sections were attached to the edge of Cu grids using Pt deposition gas in the FIB. The electron transparent FIB sections were examined using a 300 keV Philips CM300 field emission transmission electron microscope (TEM) equipped with an Oxford Instruments solid-state energy-dispersive X-ray (EDX) spectrometer, EmiSPEC spectral processing software, and Digital Micrograph (ver. 3.3.1) imaging software. Bright-field and dark-field imaging, electron diffraction, and EDX spectroscopy were used to investigate compositions and mineralogy of the extracted sections. All images were recorded using a slow-scan charge-coupled–device (CCD) camera (2048×2048 pixels).

2.3. Infrared Spectroscopy

Laboratory infrared spectroscopy can not only examine the structure of a material, but more importantly, it also allows for comparison with astronomical observations. While the infrared spectra of crystalline materials are typically dominated by a few well-defined narrow bands, amorphous materials are characterized by broad and structureless bands (Dorschner 1999; Jaeger et al. 1998). In the present study, we examined the ion-irradiated samples using IR reflection spectroscopy. The infrared measurements were made using an attenuated total infrared reflectance (ATR) in a Thermo-Nicolet 670 Nexus Spectrometer operating at 4 cm^{-1} resolution. The beam path and sample compartment were purged continuously with dry air. The ATR used a ZnSe substrate and an angle of incidence of 45°. The reflectance was normalized to the total reflectance of the ZnSe prism without a sample. The sampling depth was less than ~ 2 μm. Note that since the index of refraction of crystalline forsterite in the 10–12 μm region is even higher than that of ZnSe, the spectra appear different from what would be expected in a transmission experiment. ATR measurements of the samples taken 1 month after irradiation and repeated ~ 5–6 months after irradiation produced the same ATR spectra within errors.

3. RESULTS

Astronomical IR data demonstrate unambiguously that crystalline silicates are the magnesium-rich end-members olivine (forsterite; Mg_2SiO_4) and pyroxene (enstatite; $MgSiO_3$) (Sylvester et al. 1999; Molster et al. 2002a, 2002b, 2002c; Waters 2004). This study is focused on the irradiation effects in forsterite; we expect that enstatite with a similar composition will behave similarly. The RBS/C spectra of irradiated forsterite samples show a progressive increase in the RBS/C yield with increasing fluence (Figure 1a), which is due to amorphization, revealed by TEM and infrared absorption spectroscopy data discussed below. If we assume that each ion forms a cylindrical track of amorphous material along its path, full amorphization of the near-surface layer is reached as the fluence increases, and the tracks overlap. Using the model described in § 2.1 (Gibbons 1972), we derive an effective track radius of (2.8 ± 0.6) nm (Fig. 1b).

TEM studies revealed that the sample was amorphized up to a depth nearly half the projected ion range (2400 nm; Ziegler 2003) at a fluence of 3×10^{13} ion^{-1} cm^{-2}, as shown in Figures 2a–2b. TEM results are similar to previous reports for ion-induced amorphization of SiO_2 in the electronic collision regime (Meftah et al. 1994) and of enstatite at the border of electronic and elastic
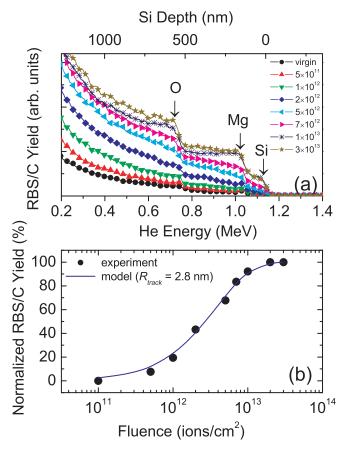
FIG. 1.—(*a*) Selected RBS/C spectra illustrating the accumulation of lattice disorder in forsterite single crystals irradiated with 10 MeV Xe ions at room temperature at different fluences, as indicated in the legend (in ions cm^{-2}). The spectrum for a fluence of 3×10^{13} ions cm^{-2} coincides with the random spectrum. (*b*) Normalized RBS/C yields fit to a track-overlap amorphization model (Gibbons 1972) giving an effective ion track radius of 2.8 nm.

FIG. 2.—Cross-sectional bright-field (*a*) and dark-field (*b*) TEM images of single crystal forsterite irradiated at room temperature with 10 MeV Xe ions to a dose of 3×10^{13} ions cm^{-2}. (*c*) and (*d*) Selected-area electron diffraction patterns taken from the left and right parts of the specimen, respectively, confirming the ion-induced structural modification from the initial single crystal to a completely amorphous material.

collision regimes (Jaeger et al. 2003). Chemical analysis of the amorphous region by EDX spectroscopy and X-ray photoelectron spectroscopy did not indicate any change in composition.

ATR spectra for different ion fluences are shown in Figure 3*a*. The transition from crystalline forsterite, characterized by narrow spectral features, to an amorphous silicate structure, evidenced by a broad structureless absorption band (Jaeger et al. 2003; Brucato et al. 2004; Demyk et al. 2004), occurs at the same fluences as indicated by the RBS/C analysis in Figure 1.

4. DISCUSSION

4.1. *Amorphization by CRs in the ISM*

The rate at which crystalline silicates are amorphized in the ISM can be determined by convolving the energy-dependent flux of CRs with the "damage" level produced by ions of a given energy. We discuss this in more detail below.

4.1.1. *The Interstellar CR Spectrum*

To estimate the CR flux experienced by interstellar grains, we note that it is not sufficient to consider the high-energy CR flux (>1 GeV nucleon^{-1}) measured on Earth, since the lower energy CRs, which should dominate amorphization in the ISM, are inhibited from entering the solar system by the magnetic field in the solar wind. The CR spectrum can be described using a leaky-box model for the propagation and escape of Galactic CRs (Ip &
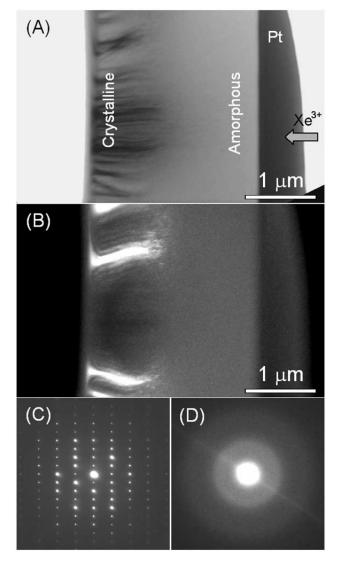
Axford 1985). The flux, $\Phi(E)$, as a function of total energy per particle, E, is then given by

$$\Phi = CE^{0.3}/(E + E_0)^3 \ (\mathrm{cm}^2 \ \mathrm{s \ sr \ GeV})^{-1}, \qquad (1)$$

where C is a constant that, as we show below, can be determined by a fit to the high-energy CR flux measured on Earth and the scaling factor E_0 sets the level of low-energy CRs (Webber & Yushak 1983).

Because molecular abundances in interstellar clouds depend ultimately on the CR ionization rate, molecular observations provide a direct handle on the low-energy CR flux (Guellin et al. 1977; Wootten et al. 1979; McCall et al. 2003). While earlier studies report CR ionization rates of 2×10^{-17} s^{-1} for molecular clouds, recent observations of H_3^+ and other species have converged on a CR ionization rate of 2×10^{-16} s^{-1} in the diffuse ISM (Tielens 2005).

Using equation (1), the primary CR ionization rate can be calculated using the differential ionization cross section (Opal
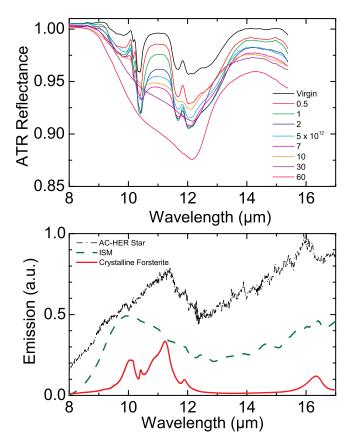
FIG. 3.—(a) ATR infrared spectra of forsterite samples irradiated at different fluences, as indicated in the legend (in cm^{-1}). (b) Astronomical emission spectra showing a broad amorphous band in the ISM (Chiar & Tielens 2005) and crystalline peaks for dust in the ejecta of the red giant, AC Her (Molster et al. 2002b) A laboratory spectrum of polycrystalline forsterite (Koike et al. 2003; see also http://www.kyoto-phu.ac.jp/labo/butsuri/data/Koike03A&A/Fo100.csv) is also shown for comparison.
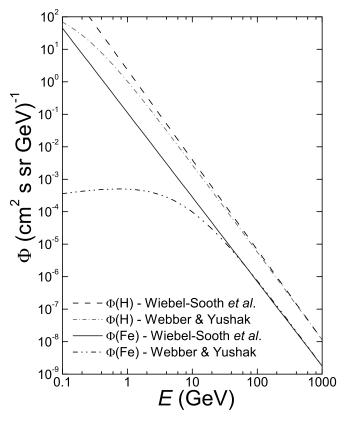

FIG. 4.—CR flux of H and Fe vs. total energy (energy per particle), for both the unmodulated (Wiebel-Sooth et al. 1998) and modulated (Webber & Yushak 1983) case. [*See the electronic edition of the Journal for a color version of this figure.*]

et al. 1972) fit to the experimental data on H$_2$ (Rudd et al. 1985). The primary CR ionization rate as a function of the scaling factor E_0 describing the low-energy CR ionization flux is then

$$\zeta_p = 5.85 \times 10^{-16}(E_0/100 \text{ MeV})^{-2.56} \text{ s}^{-1} \text{ (H nuclei)}^{-1}.$$

Hence, the molecular observations imply $E_0 \sim 120$ MeV for H.

The value $C = 1.45$ (cm^2 s sr GeV$^{-1.7}$)$^{-1}$, was obtained by matching equation (1) to experimental data at high energies (e.g., $E = 1$ TeV particle^{-1}; Wiebel-Sooth et al. 1998), where modulation by the solar wind has no influence. The high-energy data for protons were taken as Φ(cm^2 s sr GeV)$^{-1}$ = $\Phi_0[E(\text{GeV})/(1000 \text{ GeV})]^{-\gamma}$, with $\Phi_0 = 11.51 \times 10^{-9}$(cm^2 s sr GeV)$^{-1}$ and $\gamma = 2.77$ (Wiebel-Sooth et al. 1998).

The flux of Fe CR responsible for amorphization of interstellar silicates is then provided by equation (1), with E_0 equal to 56×0.12 GeV particle^{-1} = 6.72 GeV particle^{-1} and $C = 8.16 \times 10^{-4}$(cm^2 s sr GeV$^{-1.7}$)$^{-1}$. Here, C was obtained as for the H flux by matching equation (1) to experimental data at $E = 1$ TeV, with $\Phi_0 = 1.78 \times 10^{-9}$(cm^2 s sr GeV)$^{-1}$ and $\gamma = 2.6$ (Wiebel-Sooth et al. 1998). This gives a Fe flux that is $\sim 5.6 \times 10^{-4}$ smaller than the H flux. Using earlier experimental data, Leger et al. (1985) assumed a factor of $\sim 1.6 \times 10^{-4}$ between the H and Fe fluxes, which would give a slightly lower total Fe flux. Figure 4 shows the resulting H and Fe flux.

4.1.2. *Amorphization by Ions at Interstellar CR Energies*

While the ion energies in our experiments (0.08 MeV nucleon^{-1}) are in the electronic energy regime, they are lower than relevant CR energies (1–100 MeV nucleon^{-1}). However, based on models for ion damage in solids, validated by experiments on high-energy irradiation of quartz, we can extrapolate our results to the ISM. We have fit the experimental results for several ions bombarding quartz (Meftah et al. 1994) to two analytical phenomenological models (Szenes 1997; Tombrello 1994) for track size versus stopping power.

At keV energies, the energy deposition is dominated by elastic atom-atom collisions. At MeV energies and above, corresponding to CRs, energy deposition is mostly due to electronic excitations. Specifically, heavy CRs create nanometer-sized tracks of dense electronic excitations that can be (partly) converted into atomic motion (Bringa & Johnson 2004; Berthelot et al. 2000; Toulemonde et al. 2002; Szenes 1997; Tombrello 1994; Meftah et al. 1994) and can lead to amorphization in a cylinder of the material forming the track. For ion energies typical for CRs, the cross section to create electronic excitations increases with increasing ion mass (Ziegler 2003).

To extrapolate the track size measured for 10 MeV Xe atoms to astrophysically relevant ions and energies, we have used both the "thermal-spike" model proposed by Szenes (1997) and the bond-breaking model by Tombrello (1994). We calculated dE/dx versus E for both Xe and Fe using the SRIM2003 code (Ziegler 2003) for a forsterite density of 3.2 g cm^{-3}. Therefore, (dE/dx) and $R_{\text{track}}(dE/dx)$ are both known as functions of projectile energy. As shown in Figure 5, these models, although formulated differently, predict roughly the same size for the amorphous
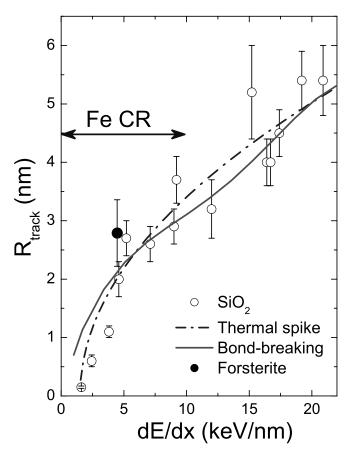
Fig. 5.—Amorphous track radius vs. electronic stopping power dE/dx. Experimental data points are for forsterite (this work) and quartz (Meftah et al. 1994). The lines are results of the thermal spike (Szenes 1997) and bond-breaking (Tombrello 1994) model predictions. The dE/dx range for 0.1–10 GeV Fe CRs in forsterite is also shown. [See the electronic edition of the Journal for a color version of this figure.]

track. The semianalytic model by Toulemonde et al. (2002) also gives similar results. All these models are expected to give poor results at low dE/dx, close to the threshold for track formation, but still agree within a factor of 2 with the experimental data in this dE/dx range. Given that the track size in pure SiO_2 scales fairly well with $(dE/dx)_{elec}$ alone (as shown in Fig. 5), we expect roughly the same amorphous track radius for the same dE/dx for any ion, including Fe ions. We note that the data in Figure 5 are for a variety of ions in the range $\sim$0.01–3.6 GeV and that its dispersion might be partly due to the "velocity effect" (Meftah et al. 1994), i.e., two different ions with the same dE/dx (but different velocity) produce somewhat different track sizes. Even taking into account this dispersion, one can notice the reasonably good agreement between the different models and experiments, including our results on forsterite, despite the much higher chemical complexity compared to SiO_2. This agreement supports our extrapolation of the track radius to the higher CR energies in the ISM.

4.1.3. The Interstellar Amorphization Timescale

For a given ion energy E, there is a flux $4\pi\Phi(E)$ on each grain. Each ion creates an amorphous track of area πR_{track}^2, which depends on the incident energy through $dE/dx(E)$. The amorphization time, Δt_{amorph}, of a grain can be estimated as

$$\Delta t_{amorph} = \left[\int_{E_{min}}^{E_{max}} 4\pi^2 R_{track}^2 \Phi(E) \, dE \right]^{-1}. \qquad (2)$$

It is possible to integrate over multiple CR species, besides Fe, with dE/dx high enough to produce amorphous tracks, but the flux of these other species is negligible and would not significantly change the amorphization time calculated for Fe alone. For submicron grains, even the less energetic CR (at E_{min}) will produce an amorphous track across the whole grain. In this limit, Δt_{amorph} is independent of the grain area. Equation (2) neglects any track overlap, but including it based on a model (Gibbons 1972; see also our Fig. 1b) further increases the amorphization time by up to a factor of $\sim$4. This is the number we report below.

Note that the minimum kinetic energy for a CR escaping from a supernova remnant shock, E_{min}, can be fixed by requiring that it be at least larger than $2mv_{shock}^2$, where m is the mass of the particle and v_{shock} is the shock velocity (Bell 1978). For shock velocities of order 10^3–10^4 km s^{-1}, E_{min} is in the range 5.2 keV to 0.52 MeV for a proton, and correspondingly larger for heavier ions. For Fe CR, $E_{min} \sim$ 0.29–29 MeV. Since no tracks form in thin layers for $E > 5$ GeV [$(dE/dx) < 1.5$ keV nm^{-1}], we use $E_{max} = 5$ GeV. Using the flux described above for $E_{min} = 0.03, 0.1,$ and 1 GeV gives $\Delta t_{amorph} \sim 65, 68.5,$ and 180 Myr, respectively. These times correspond respectively to $\sim$233, 230, and 180 Fe CR impacts every million years on a grain of 0.1 μm radius.

4.1.4. The Fraction of Interstellar Crystalline Silicates

Based on our experiments, we have calculated an exposure time of nearly 70 Myr to completely amorphize crystalline silicates in the ISM. To evaluate quantitatively the crystalline silicate fraction in the ISM, we develop a simple model following McKee (1989) and Kemper et al. (2004). Amorphous and crystalline silicate grains are injected into the ISM by stars in the later stages of their evolution and destroyed by sputtering in strong shock waves driven by supernova explosions. In addition, dust is lost when new stars are formed. The last process to consider is the amorphization of crystalline grains by CRs. In steady state, the crystalline-to-amorphous mass fraction, δ, is then given by

$$\delta = (k_{SF} + k_d)[k_{CR}(1 + \delta_0) + k_{SF} + k_d]^{-1}\delta_0$$

under the assumption that sputtering destroys crystalline and amorphous silicates at the same rate. Here, k_{SF} is the star formation rate (2×10^{-10} yr^{-1}, corresponding to 1 $M_\odot$ yr^{-1}; McKee 1989), k_d is the dust destruction rate (2.5×10^{-9} yr^{-1}, corresponding to silicate lifetime of 4×10^8 yr; Jones et al. 1996), k_{CR} is the amorphization rate (1.4×10^{-8} yr^{-1}, corresponding to 7×10^7 yr; this work), and δ_0 is the fraction of silicates injected into the ISM in crystalline form. With these values, this equation simplifies to

$$\delta \sim (k_d/k_{CR})\delta_0.$$

Estimates for δ_0 vary from $\sim$0.15 if AGB stars dominate the dust budget to $\sim$0.05 if supernovae are important sources of amorphous silicates (Kemper et al. 2004). The estimated fraction of crystalline silicates ranges then from 0.008 to 0.027, which should be compared to the observed fraction of less than $\sim$0.01 (Kemper et al. 2004).

4.2. Amorphization by Ion Bombardment in Interstellar Shocks

As mentioned in the introduction, several studies have shown silicate amorphization by H and He ions at 4–50 keV at fluences representative of fast shocks in the diffuse ISM. However, the volume of a grain affected by keV ion irradiation is to first order set by the range of the ion. To fully amorphize a grain of 0.1 μm radius, H (He) ions require an energy of 10 (15) keV (Ziegler

2003), corresponding to a $\sim$1400 (850) km s^{-1} shock. In a two-phase ISM, a single supernova remnant irradiates dust in the equivalent of $\sim$60 $M_\odot$ of interstellar gas with shocks of velocities exceeding 1000 km s^{-1} (McKee 1989). With a total ISM gas mass of 4.5×10^9 $M_\odot$ and an effective supernova rate of 8×10^{-3} yr^{-1}, the timescale to amorphize is 10^{10} yr (McKee 1989). Therefore, high-velocity shocks would not amorphize dust grains efficiently.

4.3. *The Life Cycle of Crystalline Silicates*

The life cycle of interstellar dust starts with the nucleation and growth of high-temperature condensates such as silicates at high densities and temperatures in the ejecta from stars, such as AGB stars and supergiants. This ejecta is rapidly mixed with other gas and dust in the ISM. A dust grain cycles many times between the intercloud and cloud phases until it is either destroyed by fast supernova shocks or incorporated into newly formed stars or planetary systems. Observations with the *Infrared Space Observatory* have revealed that crystalline silicates are abundant in the initial stages of this life cycle, the ejecta from stars, as well as in last stages, circumstellar disks around Herbig AeBe stars and T Tauri stars, but are absent in the intermediate stages (Sylvester et al. 1999; Kemper et al. 2004; Malfait et al. 1998; Waters & Waelkens 1998). As our experimental and modeling results demonstrate, crystalline silicates injected into the ISM can be rapidly amorphized by Galactic CRs on a timescale that is short compared to other relevant timescales (§ 4.1.3). The high abundance of crystalline silicates in circumstellar disks surrounding young stars (Waters & Waelkens 1998) must then reflect subsequent processing of grains in these environments. Recent mid-infrared spectroscopic interferometry on AU scale sizes has revealed the presence of a strong gradient in the crystallinity of silicates in the circumstellar disks of the three objects investigated (van Boekel et al. 2004). This likely reflects the rapid annealing in the hot inner regions of these disks coupled with turbulent diffusion outward of the crystalline grains.

Parenthetically, we mention here that presolar SiC grains recovered from meteorites at the parts per million level are generally crystalline. These grains are formed in the ejecta of AGB stars and other stellar dust sources and after a long and harsh sojourn in the ISM became part of the solar nebula and eventually the parent body of meteorites. While our experiments do not directly pertain to SiC, this material should also amorphize by high-energy ion bombardment. These grains are larger than 10 μm and are therefore larger than typical interstellar grains, and it is unknown whether they were incorporated into meteorites as individual SiC grains or as components of even larger multi-mineral grains. The extent to which they have been modified after accretion into the meteorite parent body is also unknown, but recrystallization by thermal annealing in the solar nebula is possible.

4.4. *Amorphization of Grains in the Solar System*

Crystalline silicates are an abundant component of dust from comets. Likewise, interplanetary dust particles (IDPs) collected in the stratosphere contain silicates (Bradley et al. 1992; Bradley 2004). It is thus of interest to consider the amorphization of crystalline silicates in the solar system. IDPs are part of the zodiacal dust, a tenuous disk of small (1–200 μm) dust particles orbiting within 5 AU of the Sun. The lifetime of these particles due to the Poynting-Robertson drag has been calculated to be $\sim$10^5 yr (Fixsen & Dwek 2002). Direct estimates of IDP residence times in the solar system have been obtained from ob-

servations of implanted solar flare tracks densities and measurements of Galactic and solar CR-generated radionuclides (Bradley et al. 1984; Nishiizumi et al. 1991). These lifetimes are shorter than the timescale against complete amorphization of micron-sized silicates by Galactic CRs derived in § 4.1.3, even more so if we consider that low-energy CRs are excluded from the solar system by the solar wind.

4.5. *Amorphization of Grains in Debris Disks*

More than 15% of all main-sequence stars have a debris (or dusty) disk (Habing et al. 1999; Lagrange et al. 2000). A-type stars do not have stellar winds, and hence, the interstellar CR-induced crystallization lifetime calculated in § 4.1.3 can be compared to the dust lifetime in these systems. We estimate the lifetime against the Poynting-Robertson drag as $\sim$10^5 yr for an A-type star with $M_* = 3$ $M_\odot$. These grains will thus not be amorphized by Galactic CRs over their lifetime. Grains dynamically trapped in a resonance with an orbiting planet (Kalas et al. 2005) can be much older and amorphized on a timescale of $\sim$70 Myr by Galactic CRs, which could be revealed by infrared spectroscopy of this dust. However, if the lifetime of the system is limited, e.g., β Pictoris, which is estimated to have an age of only 12 Myr, amorphization will not have proceeded very far yet, even for dynamically trapped grains.

5. CONCLUSION

Our experimental irradiation studies show that crystalline silicates are readily amorphized by swift heavy ions, in agreement with previous studies on SiO$_2$ (Meftah et al. 1994). Using theoretical models, we extrapolated these experimental results to astrophysically relevant energies to show that cosmic rays with energies between 0.1 and 5 GeV will amorphize crystalline silicate grains in the ISM on a timescale of 70 Myr. This timescale is much shorter than that between the injection of silicate materials into the ISM by old stars and their incorporation into new stars and planetary systems ($\sim$2500 Myr; Savage & Sembach 1996), and the destruction of silicates in the ISM (400 Myr; Jones et al. 1996). We estimate that, in steady state, less than 0.3% of the crystalline grains injected into the ISM survive amorphization. This is qualitatively consistent with the observed interstellar abundance of crystalline silicates (Kemper et al. 2004) as well as the abundance of (isotopically anomalous) presolar crystalline silicates in meteorites and IDPs (Messenger et al. 2003; Floss et al. 2006).

The IR spectra of irradiated silicates lose the narrow features characteristic of crystalline materials and develop a broad featureless band in the 10–12 μm region. This spectral change due to amorphization parallels the emission spectral differences between silicates ejected by old stars and silicate grains observed in the ISM. Thus, CR irradiation of interstellar silicates affects the opacity of the ISM.

In addition, we have examined the irradiation of silicates in the solar system and in debris disks. For the solar system, CR irradiation of zodiacal dust will have little effect, since the Poynting-Robertson drag severely limits the grains' lifetime in the inner solar system. Amorphization of debris disks around A-type stars by CRs is also similarly limited by the Poynting-Robertson drag, unless the dust is trapped in long-lived resonances with planetary companions. Infrared spectroscopic studies of such systems may provide information on the lifetime of these grains.

We note that other consequences of CR irradiation are the destruction of small grains (Bringa & Johnson 2004) and the synthesis and ejection of complex molecules formed on the grain surface. CRs will also restructure the grain surfaces, which may

affect the formation efficiency of H_2 as suggested by Monte Carlo simulations revealing that the temperature range for high-efficiency H_2 formation is larger for heterogeneous than for crystalline surfaces (Cuppen & Herbst 2005). Since we find that the amorphization timescale is so short, nearly all dust grains in the ISM will have been processed, and the H_2 and subsequent star formation will be maximized (i.e., *positive* feedback).

Energetic ion impacts may have been particularly important in the early universe during the formation and co-evolution of galaxies and their central galactic black holes (Di Matteo et al. 2005; Silk & Rees 1998). Those environments are characterized by both rapid injection of freshly synthesized (crystalline) silicates by short-lived massive stars as well as high supernova rates (e.g., high CR fluxes) and jets of energetic particles from the central black hole. The crystalline-to-amorphous silicate fraction in these environments is then a balance between the injection and the amorphization process, and based on our experimental and theoretical studies, observations could then be used to deduce the flux of energetic particles in these environments, which is hard to determine otherwise.

Recently, the spectroscopic signature of crystalline silicate was recognized in the spectra of a sample of deeply embedded ultraluminous infrared galaxies (ULIRGs; Spoon et al. 2006). This class of ULIRGs likely reflects a brief, early phase in the evolution of ULIRGs in which star formation and active galactic nucleus (AGN) activity had not yet had time to process and disperse the nuclear gas and dust. The presence of copious amounts of crystalline silicates in these starburst environments suggests that the dust has been injected very recently (<70 Myr), presumably by massive stars formed in the star burst and, therefore, has not yet been amorphized by CR ions. This is consistent with ULIRG starburst age estimates of 10–100 Myr (Genzel et al. 1998).

REFERENCES

Bell, A. R. 1978, MNRAS, 182, 443
Berthelot, A., et al. 2000, Phil. Mag. A, 80, 2257
Bradley, J. P. 2004, in Treatise on Geochemistry 1, ed. A. Davis, H. D. Holland, & K. K. Turekian (Amsterdam: Elsevier), 689
Bradley, J. P., Brownlee, D. E., & Fraundorf, P. 1984, Science, 226, 1432
Bradley, J. P., Humecki, H. J., & Germani, M. S. 1992, ApJ, 394, 643
Bringa, E. M., & Johnson, R. E. A. 2004, ApJ, 603, 159
Brucato, J. R., Strazzulla, G., Baratta, G., & Colangeli, L. A. 2004, A&A, 413, 395
Chiar, J., & Tielens, A. G. G. M. 2006, ApJ, 637, 774
Chu, W. K., Mayer, J. W., & Nicolet, M. A. 1978, Backscattering Spectroscopy (New York: Academic)
Cuppen, H. M., & Herbst, E. 2005, MNRAS, 361, 565
Day, K. L. 1977, MNRAS, 178, P49
Demyk, K., d'Hendecourt, L., Leroux, H., Jones, A. P., & Borg, J. 2004, A&A, 420, 233
Demyk, K., et al. 2001, A&A, 368, L38
Di Matteo, T., Springel, V., & Hernquist, L. 2005, Nature, 433, 604
Dorschner, J. 1999, in Formation and Evolution of Solids in Space, ed. J. M. Greenberg & A. Li (Dordrecht: Kluwer), 229
Draine, B. T. 2003, ARA&A, 41, 241
Fixsen, D. J., & Dwek, E. 2002, ApJ, 578, 1009
Fleischer, R. L., Price, P. B., & Walker, R. M. 1975, Nuclear Tracks in Solids (Berkeley: Univ. California Press)
Floss, C., Stadermann, F. J., Bradley, J. P., Dai, Z. R., Bajt, S., & Lea, A. S. 2006, Geochim. Cosmochim. Acta, 70, 2371
Genzel, R., et al. 1998, ApJ, 498, 579
Gibbons, J. F. 1972, Proc. IEEE, 60, 1062
Graham, G., et al. 2004, Lunar Planet. Sci. Conf., 35, abs. 2044
Guelin, M., Langer, W. D., Snell, R. L., & Wootten, H. A. 1977, ApJ, 217, L165
Habing, H. J., et al. 1999, Nature, 401, 456
Hollenbach, D., & Salpeter, E. E. 1971, ApJ, 163, 155
Ip, W.-H., & Axford, W. I. 1985, A&A, 149, 7
Jaeger, C., Fabian, D., Schrempel, F., Dorschner, J., Henning, Th., &. Wesch, W. 2003, A&A, 401, 57
Jaeger, C., Molster, F. J., Dorschner, J., Henning, Th., Mutschke, H., & Waters, L. B. F. M. 1998, A&A, 339, 904
Jones, A. P., Tielens, A. G. G. M., & Hollenbach, D. 1996, ApJ, 469, 740
Kalas, P., Graham, J. R., & Clampin, M. 2005, Nature, 435, 1067
Kemper, F., Vriend, W. J., & Tielens, A. G. G. M. 2004, ApJ, 609, 826 (erratum 633, 534 [2005])
Koike, C., Chihara, H., Tsuchiyama, A., Suto, H., Sogawa, H., & Okuda, H. 2003, A&A, 399, 1101
Lagrange, A.-M., Backman, D. E., & Artymowicz, P. 2000, Protostars and Planets IV, ed. V. Mannings, A. P. Boss, & S. S. Russell (Tucson: Univ. Arizona Press), 639

Leger, A., Jura, M., & Omont, A. 1985, A&A, 144, 147
Malfait, K., Waelkens, C., Waters, L. B. F. M., Vandenbussche, B., Huygen, E., & de Graauw, M. S. 1998, A&A, 332, L25
McCall, B., et al. 2003, Nature, 422, 500
McKee, C. F. 1989, in IAU Symp. 135, Interstellar Dust, ed. L. J. Allamandola & A. G. G. M. Tielens (Dordrecht: Kluwer), 431
Meftah, A., et al. 1994, Phys. Rev. B, 49, 12457
Messenger, S., Keller, L. P., Stadermann, F. J., Walker, R. M., & Zinner, E. 2003, Science, 300, 105
Molster, F. J., Waters, L. B. F. M., & Tielens, A. G. G. M. 2002a, A&A, 382, 222
Molster, F. J., Waters, L. B. F. M., Tielens, A. G. G. M., & Barlow, M. J. 2002b, A&A, 382, 184
Molster, F. J., Waters, L. B. F. M., Tielens, A. G. G. M., Koike, C., & Chihara, H. 2002c, A&A, 382, 241
Molster, F. J., et al. 1999, Nature, 401, 563
Nishiizumi, K., Arnold, J. R., Fink, D., Klein, J., & Middleton, R. 1991, Earth Planet. Sci. Lett., 104, 315
Opal, C. B., Beaty, E. C., & Peterson, W. K. 1972, Atomic Data, 4, 209
Rudd, M. F., Kim, Y. K., Madison, D. H., & Gallagher, J. W. 1985, Rev. Mod. Phys., 57, 965
Savage, B. D., & Sembach, K. R. 1996, ARA&A, 34, 279
Silk, J., & Rees, M. 1998, A&A, 331, L1
Spoon, H. W. W., et al. 2006, ApJ, 638, 759
Sylvester, R. J., et al. 1999, A&A, 352, 587
Szenes, G. 1997, Nucl. Instrum. Methods Phys. Res. B, 122, 530
Tielens, A. G. G. M. 2005, Physics and Chemistry of the Interstellar Medium (Cambridge: Cambridge Univ. Press)
Tombrello, T. A. 1994, Nucl. Instrum. Methods Phys. Res. B, 94, 424
Torres, D. F., Reimer, O., Domingo-Santamaria, E., & Digel, S. W. 2004, ApJ, 607, L99
Toulemonde, M., Assmann, W., Gruner, F., & Trautmann, C. 2002, Phys. Rev. Lett., 88, 057602
van Boekel, R., et al. 2004, Nature, 432, 479
Waters, L. B. F. M. 2004, in ASP Conf. Ser. 309, Astrophysics of Dust, ed. A. N. Witt, G. C. Clayton, & B. T. Draine (San Francisco: ASP), 229
Waters, L. B. F. M., & Waelkens, C. 1998, ARA&A, 36, 233
Watson, W. D., & Salpeter, E. E. 1972, ApJ, 174, 321
Webber, W. R., & Yushak, S. M. 1983, ApJ, 275, 391
Wiebel-Sooth, B., Biermann, P. L., & Meyer, H. 1998, A&A, 330, 389
Wootten, A., Snell, R., & Glassgold, A. E. 1979, ApJ, 234, 876
Ziegler, J. F. 2003, The Stopping Range of Ions in Matter (SRIM), Version 2003.26, http://www.srim.org